ARTICLE

Journal of Materials Chemistry
www.rsc.org/materials

Degenerate nonlinear absorption and optical power limiting properties of asymmetrically substituted stilbenoid chromophores†

Tzu-Chau Lin,[a] Guang S. He,[a] Paras N. Prasad*[a] and Loon-Seng Tan[b]

[a]*Department of Chemistry, Institute for Lasers, Photonics and Biophotonics, University at Buffalo, State University of New York, Buffalo, New York 14260-3000. E-mail: pnprasad@acsu.buffalo.edu*

[b]*Polymer Branch, AFRL/MLBP, Materials & Manufacturing Directorate, Air Force Research Laboratory, Wright-Patterson Air Force Base, Dayton, Ohio, 45433-7750*

Received 21st October 2003, Accepted 7th January 2004
First published as an Advance Article on the web 12th February 2004

Two-photon absorption (2PA) spectra (650–1000 nm) of a series of model chromophores were measured *via* a newly developed nonlinear absorption spectral technique based on a single and powerful femtosecond white-light continuum beam. The experimental results suggested that when either an electron-donor or an electron-acceptor was attached to a *trans*-stilbene at a *para*-position, an enhancement in molecular two-photon absorptivity was observed in both cases, particularly in the 650–800 nm region. However, the push–pull chromophores with both the donor and acceptor groups showed larger overall two-photon absorption cross-sections within the studied spectral region as compared to their mono-substituted analogues. The combined results of the solvent effect and the ^{1}H-NMR studies indicated that stronger acceptors produce a more efficient intramolecular charge transfer character upon excitation, leading to increased molecular two-photon responses in this model-compound set. A fairly good 2PA based optical power limiting behavior from one of the model chromophores is also demonstrated.

1. Introduction

Two-photon absorption (2PA) was theoretically predicted by Maria Göppert-Mayer in 1931,[1] the first experimental observation of this nonlinear optical phenomenon was realized about 30 years later when Kaister and Garret observed two-photon induced upconverted fluorescence emission from a CaF_2:Eu^{2+} inorganic crystal in 1961.[2] With the advent of high peak-power laser systems, some early potential applications based on multi-photon absorption phenomenon were demonstrated by Rentzepis and Parthenopoulos for optical data storage[3] and by Webb and co-workers for microscopy.[4] However, the relatively small two-photon absorption cross-sections of earlier materials limited their widespread utility. In the last decade, reports of new organic chromophores with greatly improved two-photon absorption cross-sections and up-converted fluorescence[5] have not only led to an increased interest in the development of highly efficient two-photon active materials, but also opened up numerous possibilities for new applications. These applications in photonics and biophotonics include two-photon up-conversion lasing,[6] two-photon absorption based optical power limiting and stabilization,[7] 3-D optical data storage,[3,8] two-photon excited fluorescence for nondestructive evaluation and bio-imaging,[9] and two-photon photodynamic cancer therapy.[10]

Nevertheless, the realization of the full potential of the two-photon technology still requires continuing efforts in theory, synthesis and optical characterization to provide further understanding of the structure–property relationship which can aid the development of highly active organic two-photon chromophores for practical purposes. For this reason, it is very helpful if the complete 2PA spectra for chromophores of interest can be readily obtained. In fact, very recently, the continuum-generation based 2PA spectral measurements for organic chromophore solutions have been reported by Negres *et al.*[11] In that work, a weaker continuum white-light (450–750 nm) was employed as a probe beam, in conjunction with a stronger 1210 nm laser beam as a pump beam to excite a *non-degenerate* 2PA process (nonlinear absorption of two photons with different wavelengths) in the sample medium. Another similar pump-probe experimental set-up based on picosecond continuum for the measurement of two-photon transient absorption spectra has also been reported by Oulianov *et al.*[12]

Recently, an alternative method to measure *degenerate* 2PA (nonlinear absorption of two photons with the same wavelength) spectrum by utilizing a single and powerful femtosecond white-light continuum beam has been reported.[13] The major advantage of this latter approach is that since both spectral tunability and wavelength-scanning mechanism during the measurement are not required, the entire degenerate 2PA spectrum for a given sample material can be recorded rapidly.

In this paper, we wish to present our studies of some structural parameters that contribute to enhancing the molecular two-photon absorptivities based on the selected model structures and on the new approach to measure their degenerate 2PA spectra. Simple nuclear magnetic resonance (NMR) techniques were used to rank the relative electron-withdrawing strengths of the dye acceptor groups. We also studied the solvatochromic behavior of these organic structures, which might provide information on the correlation of electron-acceptor strength and the molecular 2PA behaviors of these charge-transfer dyes. As an illustration for an application of organic two-photon materials, the optical power limiting capability of one of the model chromophores was demonstrated.

2. Model compounds

The primary objective of this study is to choose a series of model compounds and to investigate some structural parameters which may affect molecular 2PA behaviors. These parameters

† Electronic supplementary information (ESI) available: Experimental details. See http://www.rsc.org/suppdata/jm/b3/b313185h/

DOI: 10.1039/b313185h

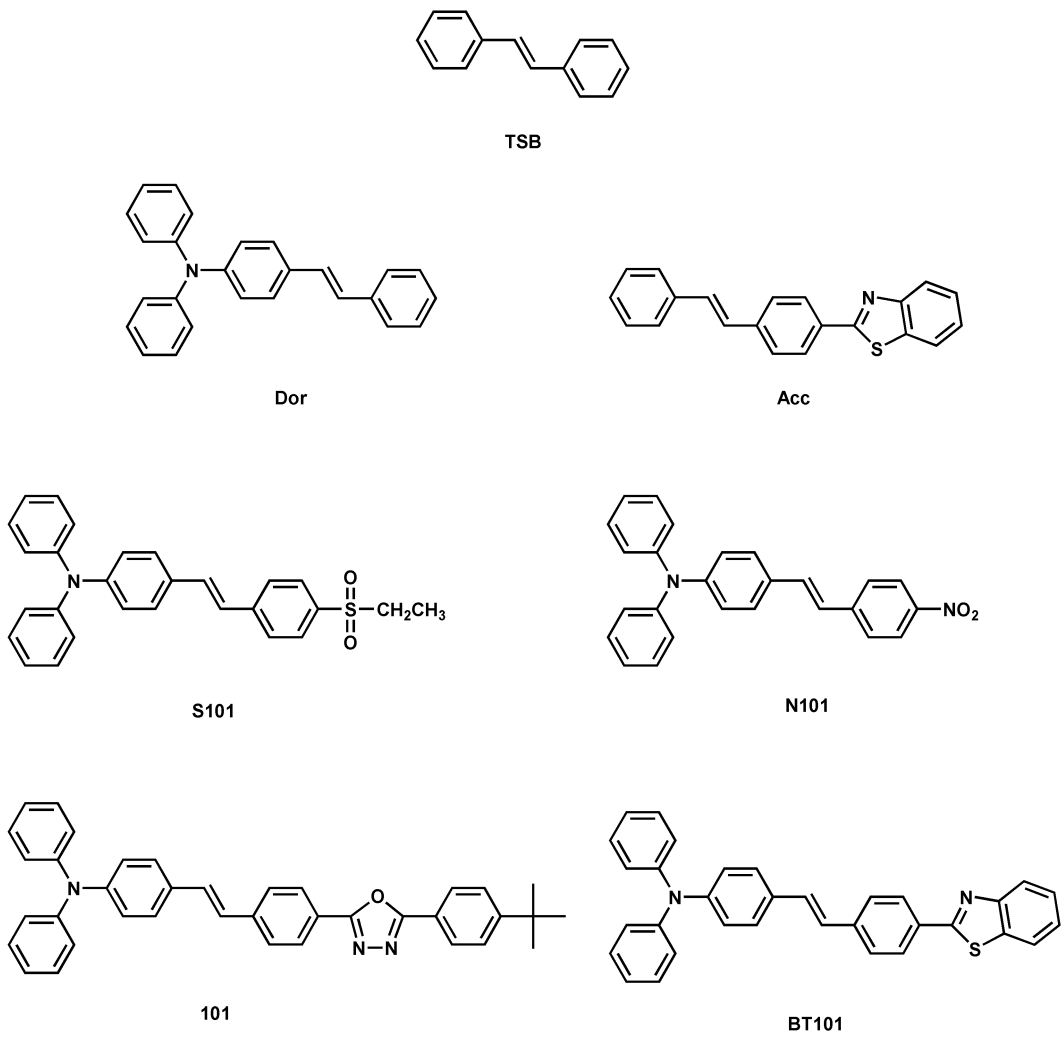

Fig. 1 Chemical structures of the selected stilbenoid chromophores studied in this work.

include (i) the contribution from the selected electron-donor (D) and/or the electron-acceptor (A) (*i.e.* push–pull effect), (ii) the contribution from the electron-withdrawing strength of the selected acceptors (*i.e.* acceptor strength effect). Based on this consideration, we have chosen *trans*-stilbene as the π-bridge, diphenylamino functional group as the donor, and four electron-withdrawing functional groups with various electron-pulling strength as the acceptors to constitute D–π, π–A, and D–π–A chromophore structures. Fig. 1 shows the chemical structures of the chosen model chromophores studied in this work.

The synthetic routes for these model chromophore molecules are briefly outlined in Schemes 1–3. All these model compounds were rigorously purified prior to characterization effort. The data for their elemental analyses and spectroscopic characterization are provided as ESI†.

3. Results and discussion

I. Optical properties characterization

Linear (one-photon) absorption spectra measurement. Linear absorption spectra of the studied model chromophores in the solution phase were measured by using a Shimadzu UV-3101PC spectrophotometer. All the sample solutions were freshly prepared in THF at a concentration of 1×10^{-5} M and filled in 1 cm path-length quartz cuvettes for this measurement. Figs. 2a and 2b show the recorded linear absorption spectra of these chromophore solutions. The linear absorption maxima of these dyes range from 296 nm to 432 nm and their extinction coefficients vary from 2360 to 5175 M^{-1} cm^{-1}. From Fig. 2a, one can see that compared to the unsubstituted *trans*-stilbene (**TSB**), both mono-substituted compounds **Dor** and **Acc** show red-shifted maximum linear absorption wavelengths which suggests that both the donor and the acceptor functional groups have a positive contribution in increasing the π-electron delocalization on the *trans*-stilbene backbone upon excitation. Furthermore, the linear absorption maximum of **Dor** is more red-shifted. This implies that the diphenylamino group is comparatively more effective in promoting π-electron delocalization than the benzothiazole moiety in this system.

From the linear absorption spectra of compounds **S101**, **101**, **BT101** and **N101** shown in Fig. 2b, we observe further red-shifted linear absorption maximum (compared to **TSB**, **Dor** or **Acc**) with the order of **S101** < **101** ~ **BT101** < **N101**, which indicates that the combination of an electron-donor and an electron-acceptor will further enhance the π-electron delocalization upon excitation in these structures.

We have measured the linear transmission spectra of these dye solutions at the same concentration (0.02 M in THF) used for the degenerate two-photon absorption spectra measurement in order to verify that no linear absorption occurs within the spectral range of 650 nm to 1300 nm. We have found that there is no linear absorption in the above-mentioned spectral range for all chromophore solutions, it follows that any intensity-dependent nonlinear absorption activities in this spectral region can be readily recorded based on the newly developed degenerate 2PA absorption spectral measurement method.[13] As an example, Fig. 3 shows the measured

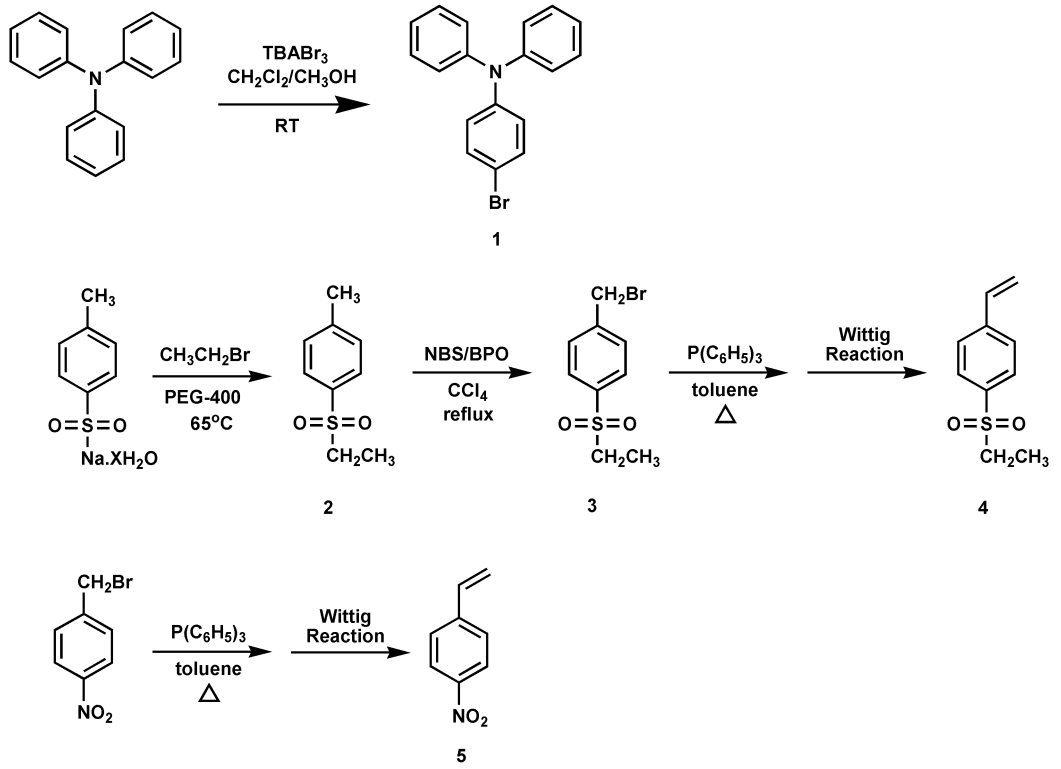

Scheme 1 Synthetic routes to the mono-brominated triphenylamine and intermediates with nitro and alkylsulfonyl functional groups.

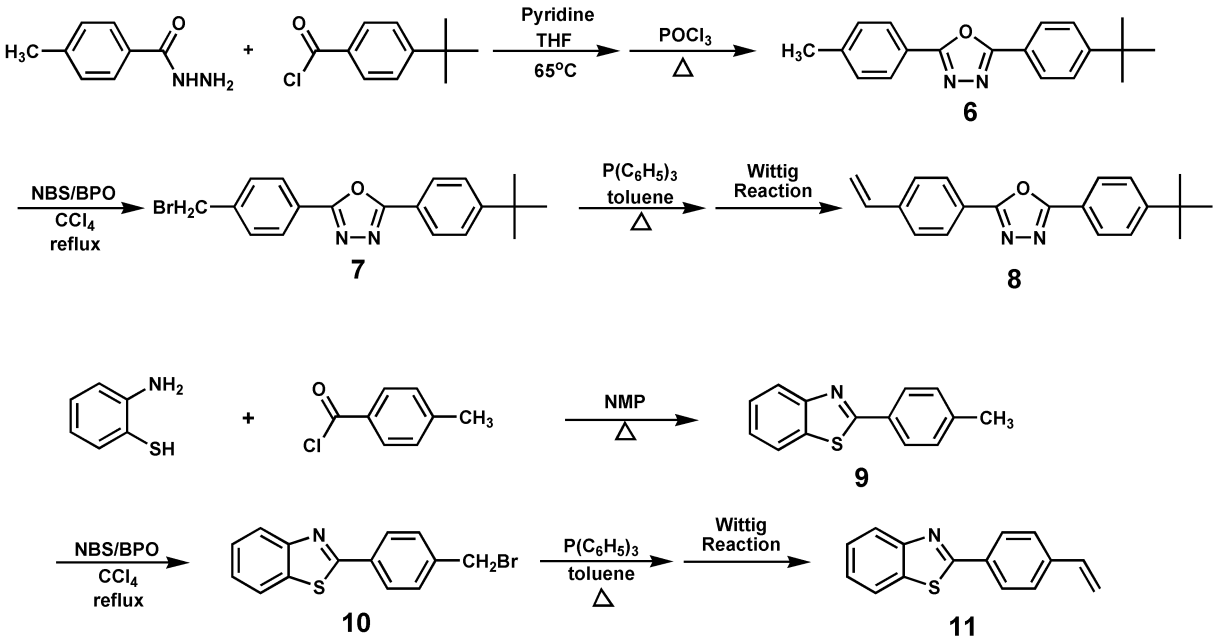

Scheme 2 Synthetic routes to the key intermediates with oxadiazole and benzothiazole functional groups.

transmission and absorption spectra of **N101** solution with high concentration (0.02 M), as this compound possesses the most red-shifted linear absorption maximum as compared to the other analogues.

Degenerate two-photon absorption (2PA) spectra measurement. Degenerate 2PA spectral measurements of these model compounds were accomplished utilizing a spectrally dispersed femtosecond white-light continuum generation from heavy water (D_2O).[13] Fig. 4 illustrates the specially designed experimental set-up for this purpose. The pump source for continuum generation was a focused ultra-short pulsed laser beam from a Ti:sapphire laser oscillator/amplifier system (CPA1, Clark-MXR ORC-1000). The pulse duration, wavelength, repetition rate and pulse energy of this pump beam were ~140 fs, ~790 nm, 1 KHz, and 150 μJ, respectively. The generated white-light continuum beam was then collimated and passed though a dispersion prism made of SF10 glass. Such a spatially/spectrally *dispersed* white-light beam was focused onto the central region of a 1 cm path-length quartz cuvette *via* an f = 10 cm lens. The quartz cuvette is either filled with the chromophore solution or the pure solvent (here in our case, the solvent is THF). With this particular experimental set-up, different spectral components of the white-light continuum beam are *spatially separated* from each other at the sample position and only *degenerate* two-photon absorption from the same spectral

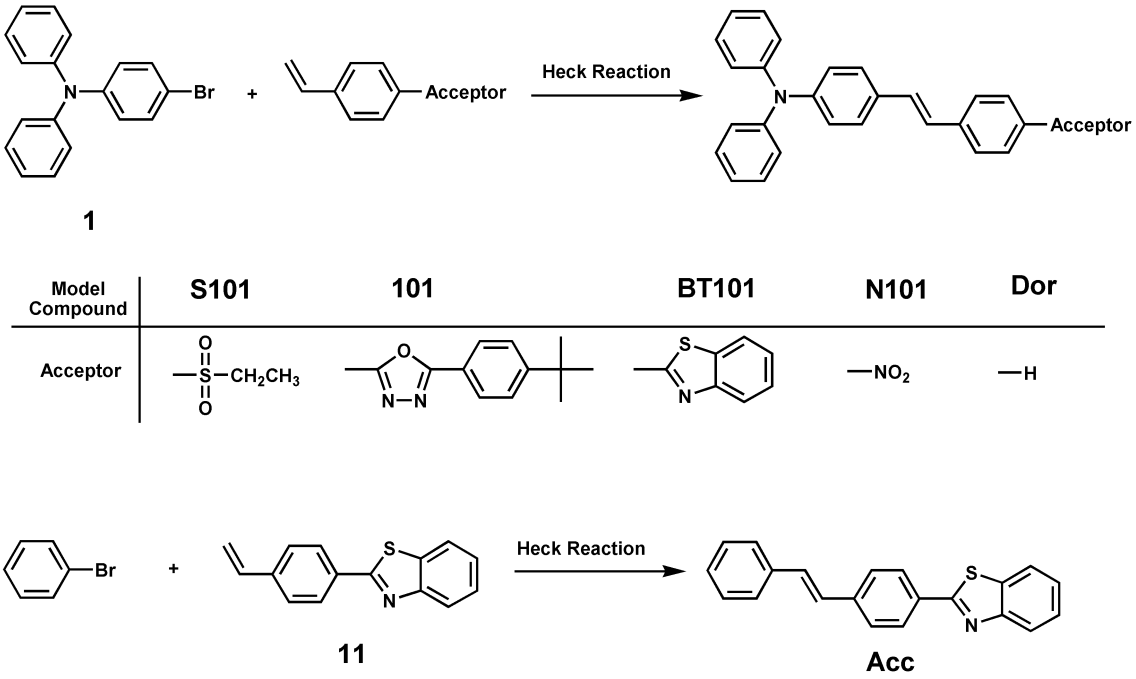

Scheme 3 Final coupling reaction procedures for the chromophore structures by following Heck reaction.

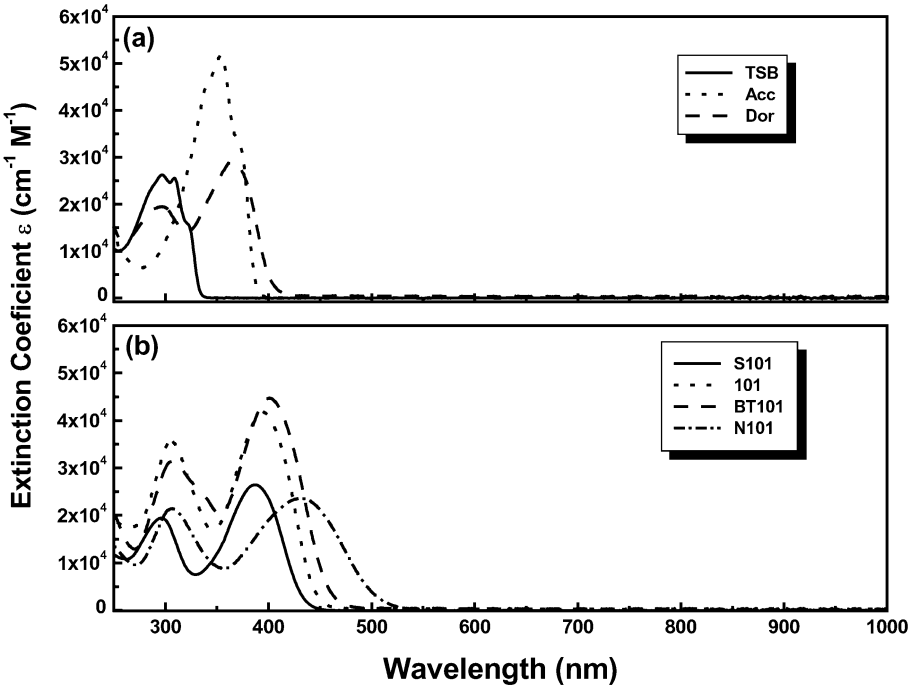

Fig. 2 Linear absorption spectra of the chromophore solutions (a) **TSB**, **Acc**, **Dor** and (b) **S101**, **101**, **BT101**, **N101** (sample solution concentration = 1×10^{-5} M; 1 cm pass-length; THF).

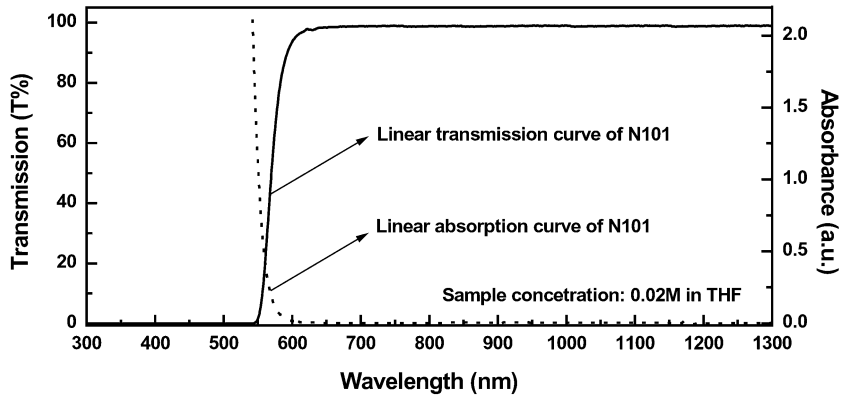

Fig. 3 Linear transmission and absorption spectra of **N101** solution at high concentration (0.02 M in THF and 1 cm path-length).

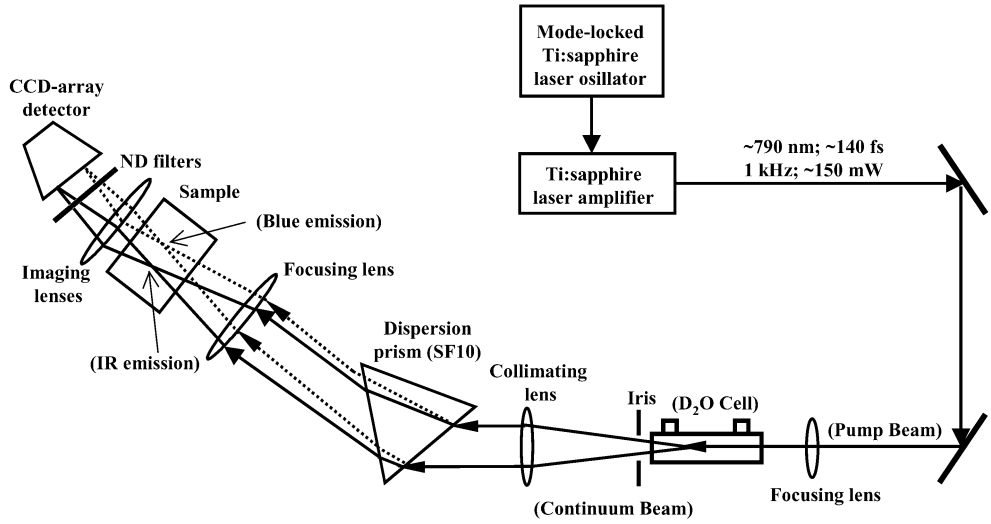

Fig. 4 Optical set-up for single femtosecond continuum beam based degenerate two-photon absorption spectral measurement.

components could take place within the sample solution. A CCD array detector was used to record the spectral intensity distribution of the transmitted continuum beam at sample position. By comparing the obtained continuum spectra profile of the sample solution with that of the pure solvent, the attenuation of different spectral components due to degenerate 2PA of the studied chromophore can be determined. This nonlinear attenuation of different spectral components provides the important information of relative 2PA cross-section values as a function of wavelengths for each chromophore, which can be finally converted into the 2PA spectrum in an absolute scale of absorption cross-section values based on a standard calibration process at a single laser wavelength.[13] Furthermore, we have optimized the input pump power level so that the intensity level of the output white-light continuum beam will not create other undesirable nonlinear optical effects[12] in the sample solution, except two-photon absorption. Fig. 5a and 5b show the measured 2PA cross-sections as a function of wavelengths for the investigated chromophore structures. The unit of the 2PA cross-section used in these figures is GM, which is defined as $1\text{GM} = 1 \times 10^{-50}$ cm^4 s per photon-molecule.

Two-photon excited fluorescence measurement. Most of the sample solutions studied manifest 2PA-induced frequency up-converted fluorescence emission. Fig 6 presents two-photon induced fluorescence spectra of compounds **S101**, **101**, **BT101** and **N101**. All the sample solutions were prepared in the same manner at concentration of 1×10^{-3} M in THF for this measurement. The excitation laser pulses of ~790 nm were

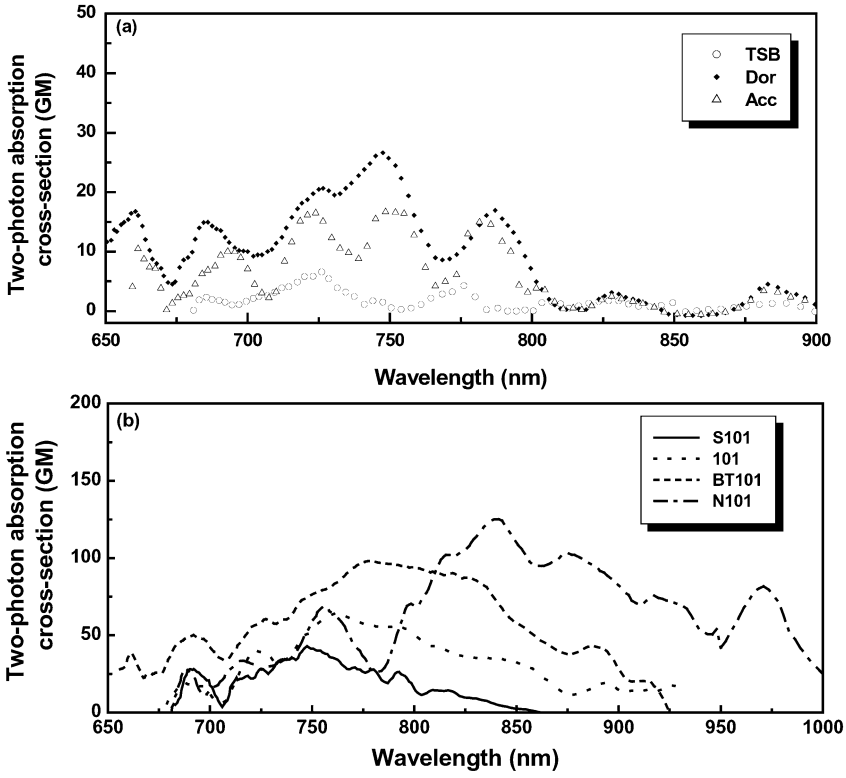

Fig. 5 (a) Measured two-photon absorption spectra of **TSB**, **Acc** and **Dor** in THF solution at 0.02 M (with experimental error ~±15%). (b) Measured two-photon absorption spectra of chromophores **S101**, **101**, **BT101** and **N101** in THF solution at 0.02 M (with experimental error ~±15%).

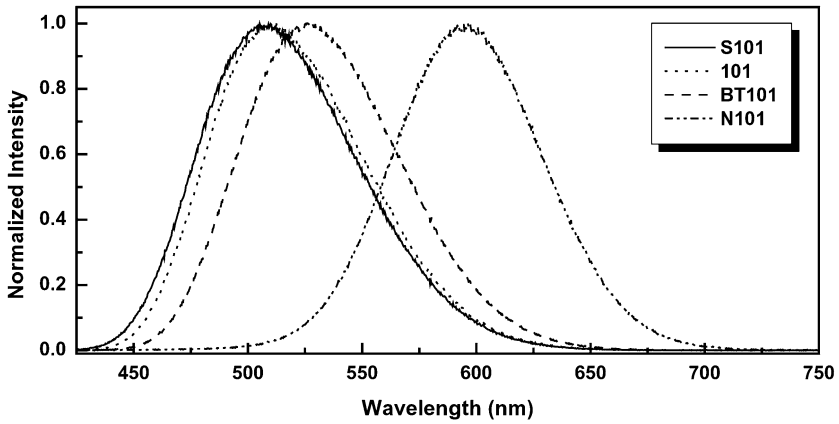

Fig. 6 Two-photon absorption (at ~790 nm) induced fluorescence emission spectra of **S101**, **101**, **BT101** and **N101** chromophore solutions at 1×10^{-3} M in THF.

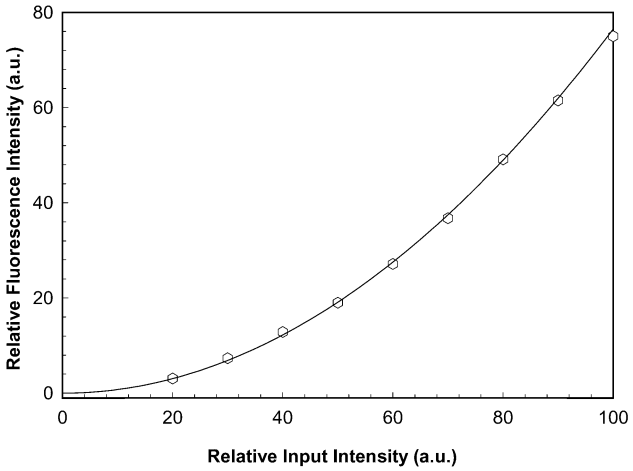

Fig. 7 Measured intensity dependence of two-photon induced fluorescence on the relative input intensity of ~790 nm laser pulses for compound **101** solution at 1×10^{-3} M in THF.

generated from the same Ti:sapphire laser oscillator/amplifier system mentioned above. The average pulse energy and the pump wavelength utilized for this measurement were ~5 μJ and ~790 nm. Fluorescence spectral measurements were accomplished by using a HoloSpec CCD-array spectrometer in conjunction with a fiber coupler head.

The dependence of the 2PA induced fluorescence intensity on the excitation intensity of these chromophore solutions were also examined. As an example, Fig. 7 shows the measured relative intensity of 2PA-induced fluorescence as a function of the input pump intensity for chromophore **101** solution at a concentration of 1×10^{-3} M. The measured data (⬡) are in good agreement with the best fitting curve following the square law, which confirms that the 2PA process is responsible for the observed up-converted fluorescence emission.

II. Relative electron-acceptor strength studies

In view of the relative simplicity and reliability of the methods to correlate the electron-withdrawing strength of the selected acceptors and the molecular 2PA behavior in this model-compound set, we have performed both ^{1}H NMR experiments (operating frequency: 400 MHz) to determine the trend for the relative electron-pulling strength of these four acceptors and solvent effect studies of these model compounds.

Proton NMR study. Table 1 presents the NMR spectral data of the aromatic proton H_a of four chosen representative structures for studying the strength of the deshielding effect from these four electron-withdrawing functional groups. It should be noted that the first three representative structures are actually the key intermediates (compounds **2**, **6**, **9**) for the synthesis toward the model chromophores, while the fourth one is purchased directly from Aldrich and used as received without further purification. It is well known that the resonance peaks of aromatic protons H_a will be shifted toward downfield in the ^{1}H NMR spectra when a stronger acceptor is attached covalently to the phenyl ring as shown in Table 1. The experimental data showed that the deshielding-strength ordering of these electron-acceptors is as follows: nitro > benzothiazole > 1,3,4-oxadiazole > alkylsulfonyl. This order parallels that of their electron-withdrawing abilities in this model set.

Similar trend of the electron-acceptor strength has been determined and reported before by G. A. Pagani and the co-workers who have employed π-charge/^{13}C NMR chemical shift relationships to study the relative electron-withdrawing

Table 1 ^{1}H-NMR chemical shift values of aromatic proton H_a influenced by different electron-acceptors

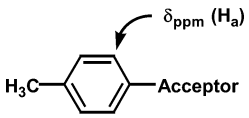

Acceptor	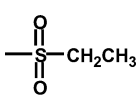	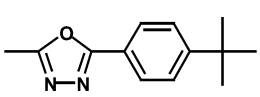	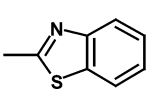	–NO_2
$\delta_{ppm}(H_a)$	7.78	8.01	8.05	8.20

Table 2 The Stokes shifts data at different solvent Δf of the studied chromophores in this work

Solvent mixture Δf[a]	$\Delta\tilde{\nu}$/cm^{-1}					
	N101	BT101	101	S101	Dor	Acc
0.0131	3884	3354	3181	3580	3062	3621
0.0058	4227	3669	3527	3898	3645	3660
0.0879	4881	3889	3712	4116	4318	3700
0.1337	5120	4397	4225	4544	4537	3739
0.1901	5639	4854	4634	4917	4067	3739
0.2099	5817	5136	4889	5136	3328	3799

[a] Orientational polarizabilities of the solvent mixture are calculated by following the equation: $\Delta f = \left[\frac{\varepsilon-1}{2\varepsilon+1} - \frac{n^2-1}{2n^2+1}\right]$, where ε is the dielectric constant and n is refractive index at 589.32 nm, which is directly obtained from ref. 18.

strength of different subsitituent groups in benzyl carbanion systems.[14]

Solvent effect study. It is well known that measuring the Stokes shift of a dye solution as a function of the orientational polarizability of the solvent is a common method to study the solvent effect based on the Lippert–Mataga equation:[15]

$$\Delta\tilde{\nu} = \frac{1}{2\pi\varepsilon_0 hc}\frac{|\Delta\mu^2|}{a^3}\Delta f + \text{Const.} \quad (1)$$

$$\Delta f = \left[\frac{\varepsilon-1}{2\varepsilon+1} - \frac{n^2-1}{2n^2+1}\right] \quad (2)$$

In this model, a chromophore molecule is treated as a dipole in a sphere of radius a within a dielectric medium (n,ε) and a linear correlation between Stokes shift ($\Delta\tilde{\nu}$/cm^{-1}), and orientational polarizability (Δf) of this dielectric medium is predicted. Solvatochromism analysis can provide a fairly good estimation of the dipole-moment change ($\Delta\mu$) of the chromophore in the solution phase upon excitation. This change in dipole moment corresponds to a distance of intramolecular charge shift along the π-bridge of chromophores upon excitation,[16] which can serve as an indication of the electron-pulling effectiveness of the selected acceptors in our dye set. In this study, we used a series of solvent-mixtures (THF–toluene) with different Δf and measured the Stokes shifts of these chromophore solutions based on their linear absorption–emission spectra.[16] The calculated values for the solvent-mixture Δf and Stokes shift are summarized in Table 2.

Based on the data collected in Table 2, we prepared Lippert plots ($\Delta\tilde{\nu}$ *vs.* Δf) for these six compounds, which are illustrated in Fig. 8. No significant deviation from the linearity, predicted by eqn. (1), was observed for any of the compounds studied here, implying that no specific interaction between the solvent and the solute in our system was involved. In our case, the experimental observation might suggest that the local molecular environment surrounding the studied chromophore consists of a uniform mixture of THF and toluene molecules *i.e.* the composition of the solvent cage surrounding the studied chromophore is roughly the same as the bulk composition and therefore, there is no significant solvent segregation occurring in the solvent cage, which may make the commonly expected preferential solvation phenomenon not very obvious. A similar observation was reported for another series of two-photon absorbing chromophores in mixed THF–hexane solvents.[17] Nevertheless, further study should be pursued in order to obtain a better understanding of the detailed solvent-solute interaction in our system. The calculated solvatochromic slopes from the linear fitting of these experimental data and other related data of these chromophores are collected in Table 3.

As mentioned above, the intramolecular charge transfer

Table 3 Solvatochromic slope, sphere radius, dipole moment change and calculated distance of charge shift data of **N101**, **BT101**, **101**, **S101**, **Dor** and **Acc**

Chromophore	Solvatochromic slope	a/Å[a]	$\lvert\Delta\mu^2\rvert$	$\lvert\Delta\mu\rvert$/D[b]	δ_d/Å[c]
N101	10070	6.44	267	16.4	3.41
BT101	9003	6.57	254	15.9	3.31
101	8642	6.53	239	15.5	3.23
S101	7830	6.47	211	14.5	3.03
Dor	7283	5.4	113	11	2.31
Acc	780	5.9	16	4	0.83

[a] This value was estimated from the optimized molecular geometry calculated with HyperChem (PM3) parameterisation. (ref. 19); [b] In the units of Debye (1D = 3.336 × 10^{-30} Cm); [c] δ_d, intramolecular charge shift. This value was calculated from $|\Delta\mu|$/4.8 D, where 4.8 D corresponds to a 1 Å separation distance of a pair of charges e and $-e$.

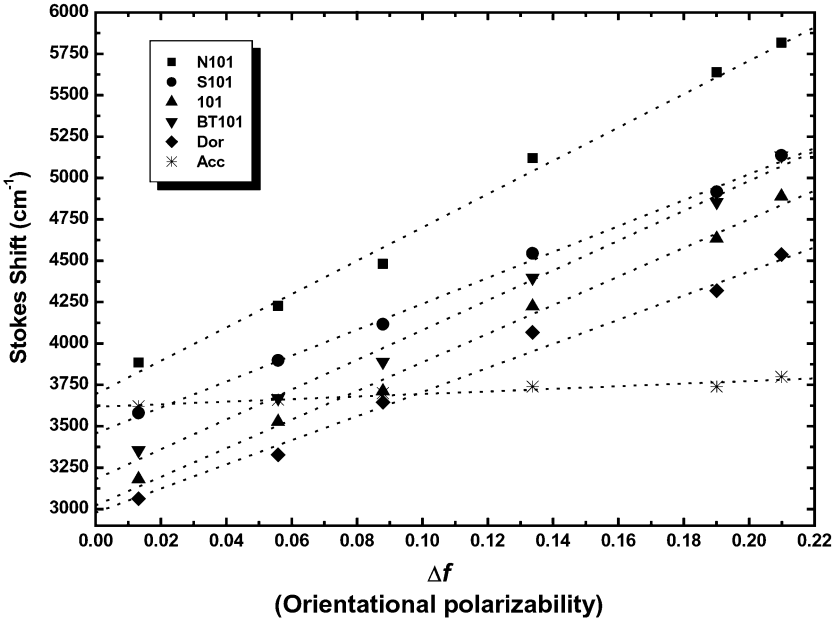

Fig. 8 Lippert plots [Stokes shift (cm^{-1}) *vs.* orientational polarity (Δf) of the solvent mixture] for chromophores **N101**, **BT101**, **101**, **S101**, **Dor** and **Acc**.

(δ_d in Table 3) of our dye molecules during the excitation can be considered as a measure of the strength of the electron-acceptors. In comparing the results of δ_d from Table 3 and δ_{ppm} from Table 1, a reasonably good agreement between these two independent experimental results confirms that the electron-pulling ability of these acceptors follows the same order. Furthermore, the "push-pull" stilbenoid structures with both the donors and the acceptors attached show larger δ_d, indicating that greater π-electron delocalization (through intramolecular charge shift) are occurring during excitation.

III. Discussion of results

From the measured linear/nonlinear optical properties and the results obtained *via* electron-acceptor strength studies of these model chromophores, the following features can be seen:

(1) In Fig. 5, with *trans*-stilbene (**TSB**) as the reference point, the slightly enhanced two-photon absorption in compounds **Dor** and **Acc** suggests that either a donor or an acceptor can contribute to the increase of the molecular nonlinear absorptivity. The attachment of both donor (diphenylamino) and acceptor (benzothiazolyl) to the **TSB** moiety has shown further enhanced molecular two-photon absorptivity (*e.g.* **BT101** *vs.* **Dor** and **Acc**). According to the results from the solvatochromic effect study (Table 3), the dipole moment change ($\Delta\mu$) values of these chromophores follows the order of **BT101** > **Dor** > **Acc**, which implies that the dipole moment change of these compounds upon excitation may have a certain effect on the enhancement of molecular two-photon absorptivity. The correlation between dipole moment change and molecular two-photon absorption has been reported in symmetrically substituted stilbenoid systems by Marder, Perry and co-workers[5a] and in that work, a concept of "charge redistribution/π-electron delocalization" has been introduced to interpret the enhanced molecular two-photon absorptivity. In our case, the nature of the D–π–A molecular structure is also suitable to promote the π-electron delocalization when excited by light, which may also increase the molecular two-photon absorptivity.

(2) The peak position of the two-photon absorption maxima of the chromophores in Fig. 5b are blue-shifted (or at significantly shorter wavelengths) compared to the wavelength positions of twice of their linear absorption maximum (*i.e.* $\lambda_{max}^{2PA} < \lambda_{max}^{1PA}$). This implies that the two-photon states with larger transition probabilities of these dye molecules are energetically above their lowest one-photon states. Similar observations have been reported for the symmetrically substituted stilbene compounds.[5a]

(3) In our model chromophore set, when stronger electron-pulling functional groups are used, a larger 2PA maximum is observed (Fig. 6), which means that the intramolecular charge transfer (or π-electron delocalization/redistribution) is important to enhance the 2PA of these model dye molecules upon excitation. Also, the 2PA peak position is red-shifted as the acceptor strength increased in this set (*i.e.* λ_{max}^{2PA} **S101**) = 748 nm; (λ_{max}^{2PA} **101**) = 761 nm; λ_{max}^{2PA} (**BT101**) = 779 nm; λ_{max}^{2PA} (**N101**) = 840 nm).

(4) In Fig. 5, non-negligible two-photon absorption at wavelengths equal to twice their linear absorption maximum positions shows that in these structures, one-photon transition allowed excited states are also accessible by two-photon transition (*i.e.* for **Dor** at 733 nm, **Acc** at 708 nm, **S101** at 773 nm, **101** at 788 nm, **BT101** at 801 nm, and **N101** at 863 nm). Moreover, it can be seen that certain detectable two-photon absorption appear at those wavelengths at which one-photon transitions are almost forbidden. This provides the evidence that excited states inaccessible by one-photon absorption can be reached by two-photon absorption. We wish to reiterate that with our experimental set-up, each component of the generated white-light beam from heavy water cells is spatially separated by the dispersion prism before interacting with the sample solution. This particular experimental arrangement also warrants that the two-photon excitation process observed here is a one-color, two-photon excitation process within the studied spectral range since there is practically no overlapping between different components of the white-light continuum.

(5) The cause of some small structures that have appeared on the measured degenerate 2PA spectra of these model compounds is not quite clear at this stage. More efforts on the understanding of solvent effects such as solvent polarity on the molecular 2PA spectral behavior and quantum-mechanical analysis of the 2PA process in this system are needed, and are under way currently.

4. Two-photon absorption based optical power limiting

It is well known that 2PA is one of the best mechanisms to achieve optical power limiting and stabilization performance.[7] For this purpose, the two-photon absorbing medium should exhibit a larger 2PA coefficient that is proportional to the concentration of the nonlinear absorbing molecules and their 2PA cross-section values. In our present study, a 2PA based optical power limiting performance was demonstrated by using a 1 cm path length solution of **BT101** in THF with a concentration of 0.04 M. Using this chromophore for optical power limiting performance is based on the fact that it possesses a relatively larger 2PA at ~800 nm wavelength position compared to other model compounds. We utilized nanosecond pulses to perform this experiment since most 2PA-based optical power limiting applications were operated within a nanosecond regime. In this regime of laser pulse duration, the excited-state absorption may contribute to a much larger effective 2PA effect that is desirable for optical power limiting applications.[7] In our experiment, as the input laser excitation source, a linearly polarized ~800 nm pulsed laser beam was provided by a dye laser system, transversely pumped by a frequency-doubled and *Q*-switched Nd:YAG laser system (Quanta-Ray Pro 230 from Spectra-Physics). The pulse duration, beam size, divergence angle, and repetition rate of the ~800 nm laser beam were ~8 ns, ~1.5 mm, ~1 mrad, and 10 Hz, respectively. After passing through an f = 15 cm lens, this laser beam was focused onto the center of the 1 cm cuvette filled with the above-mentioned sample solution. The local intensity within this sample solution can be changed by varying the incident laser power level. The transmitted laser beam from the sample cell was detected by an optical power (energy) meter with a large detection area of ~30 mm in diameter. Fig. 9a shows the measured data (○) for nonlinear transmissivity, T_i, as a function of the local intensity of the input ~800 nm laser beam. The influences from the windows of cuvette and from the solvent were eliminated by subtracting the transmission data from a pure THF-filled cuvette sample. One can see from Fig. 9a that the intensity-dependent nonlinear transmission of the sample dropped from ~0.94 to ~0.51 as the input intensity increased from ~54 MW cm^{-2} to ~652 MW cm^{-2}. In Fig. 9a, the solid-line curve is the theoretical curve predicted by the basic 2PA theory with a best fitting parameter of β = 3.14 cm GW^{-1}, where β is the effective 2PA coefficient in nanosecond regime of the sample solution. Fig. 9b shows the measured output intensity as a function of the input intensity. The experimental data are presented by open diamonds, and the solid-line curve is the theoretical curve, with the same fitting parameter of β = 3.14 cm GW^{-1}. The diagonal dash-line curve shows the behavior for a medium without nonlinear absorption for comparison. A fairly good optical power limiting behavior of **BT101** solution can be seen when the input intensity is increased from ~150 MW cm^{-2} to ~650 MW cm^{-2}.

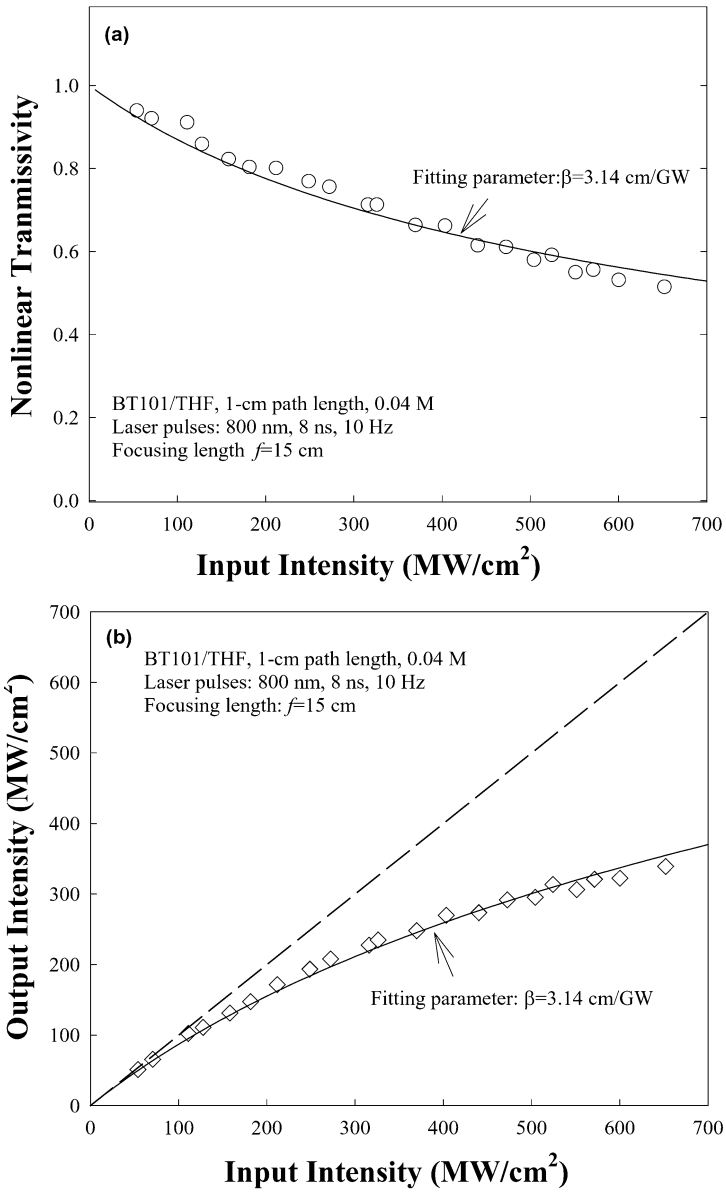

Fig. 9 (a) Measured nonlinear transmission of a 1 cm path-length **BT101** solution in THF (0.04 M) as a function of the input intensity of the ~800 nm laser beam. (b) Measured output intensity as a function of the input intensity based on the same sample solution. The solid curves are the theoretical curves with a best fitting parameter of β = 3.14 cm GW^{-1} (β is the effective 2PA coefficient).

Conclusion

We have measured the degenerate 2PA spectra by using a single and spectrally dispersed femtosecond white-light continuum as a probe tool and investigated some molecular parameter effects such as electron-donor and electron-acceptor effects on the 2PA behavior of a series of the chosen model chromophores. The results suggested that whereas either a strong electron-donor or electron-acceptor could play an important role in enhancing the molecular two-photon absorptivity in this *trans*-stilbene-based chromophore set. Asymmetric structures with both donor and acceptor appear to have more 2PA enhancement. This enhancement is increased with an increase in the electron-withdrawing strength of the acceptor. The ordering of electron-pulling strength among the acceptors used in this study can be determined by simple ^{1}H-NMR. Furthermore, in this *trans*-stilbene-based chromophore set, those structures with stronger electron-acceptors showed more efficient intramolecular charge shift/redistribution upon excitation, which is considered as one of the determinants in improving the molecular 2PA cross-sections. Using a femtosecond white-light continuum to probe molecular 2PA spectra may also have the potential to provide the important information with respect to the choice of proper operating wavelengths for a specific chromophore for nonlinear optical applications such as the optical power limiting demonstrated in this work.

Acknowledgements

This work was supported in part by the U. S. Air Force Office of Scientific Research, Washington, DC and the Polymer Branch, Materials & Manufacturing Directorate, U. S. Air Force Research Laboratory, Dayton, Ohio and in part by a grant from the Infotonic Center of Excellence, Rochester, New York. We thank Professors Mike Detty and Frank Bright of our Chemistry Department for helpful discussions.

References

1 M. Göppert-Mayer, *Ann. Phys.*, 1931, **9**, 273–295.
2 W. Kaiser and C. G. B. Garret, *Phys. Rev. Lett.*, 1961, **7**, 229–231.
3 D. A. Parthenopoulos and P. M. Rentzepis, *Science*, 1989, **245**, 843–845.
4 W. Denk, J. H. Strickler and W. W. Webb, *Science*, 1990, **248**, 73.

5 Some earlier representative examples are provided in the following references: (*a*) M. Albota, D. Beljonne, J.-L. Bredas, J. E. Ehrlich, J.-Y. Fu, A. A. Heikal, S. E. Hess, T. Kogej, M. D. Levin, S. R. Marder, D. McCord-Maughon, J. W. Perry, H. Rockel, M. Rumi, G. Subramaniam, W. W. Webb, X.-L. Wu and C. Xu, *Science*, 1998, **281**, 1653–1656; (*b*) K. D. Belfield, D. J. Hagan, E. W. V. Stryland, K. J. Schafer and R. A. Negres, *Org. Lett.*, 1999, **1**, 1575–1578; (*c*) K. D. Belfield, K. J. Schafer, W. Mourad and B. A. Reinhardt, *J. Org. Chem.*, 2000, **65**, 4475; (*d*) M. Drobizhev, A. Karotki, A. Rebane and C. W. Spangler, *Opt. Lett.*, 2001, **26**, 1081–1083; (*e*) B. A. Reinhardt, L. L. Brott, S. J. Clarson, A. G. Dillard, J. C. Bhatt, R. Kannan, L. Yuan, G. S. He and P. N. Prasad, *Chem. Mater.*, 1998, **10**, 1863–1874; (*f*) S.-J. Chung, K.-S. Kim, T.-C. Lin, G. S. He, J. Swiatkiewicz and P. N. Prasad, *J. Phys. Chem. B*, 1999, **103**, 10741–10745; (*g*) R. Kannan, G. S. He, L. Yuan, F. Xu, P. N. Prasad, A. G. Dombroskie, B. A. Reinhardt, J. W. Baur, R. A. Vaia and L.-S. Tan, *Chem. Mater.*, 2001, **13**, 1896–1904; (*h*) O.-K. Kim, K.-S. Lee, H.-Y. Woo, K.-S. Kim, G. S. He, J. Swiatkiewicz and P. N. Prasad, *Chem. Mater.*, 2000, **12**, 284–286; (*i*) A. Andronov, J. N. Frechet, G. S. He, K.-S. Kim, S.-J. Chung, J. Swiatkiewicz and P. N. Prasad, *Chem. Mater.*, 2000, **12**, 2838–2841.

6 (*a*) G. S. He, C. F. Zhao, J. D. Bhawalkar and P. N. Prasad, *Appl. Phys. Lett.*, 1995, **67**, 3703–3705; (*b*) G. S. He, J. D. Bhawalkar, C. F. Zhao, C.-K. Park and P. N. Prasad, *Opt. Lett.*, 1995, **20**, 2393–2395; (*c*) G. S. He, J. D. Bhawalkar, C. F. Zhao and P. N. Prasad, *IEEE J. Quantum Electron.*, 1996, **32**, 749–755; (*d*) G. S. He, L. Yuan, Y. Cui, M. Li and P. N. Prasad, *J. Appl. Phys.*, 1997, **81**, 2529–2537; (*e*) A. Abbotto, L. Beverina, R. Bozio, S. Bradamante, C. Ferrante, G. A. Pagani and R. Signorini, *Adv. Mater.*, 2000, **12**, 1963–1967.

7 (*a*) G. S. He, R. Gvishi, P. N. Prasad and B. A. Reinhardt, *Opt. Commun.*, 1995, **117**, 133; (*b*) G. S. He, J. D. Bhawalkar, C. F. Zhao and P. N. Prasad, *Appl. Phys. Lett.*, 1995, **67**, 2433–2435; (*c*) G. S. He, L. Yuan, N. Cheng, J. D. Bhawalkar, P. N. Prasad, L. L. Brott, S. J. Clarson and B. A. Reinhardt, *J. Opt. Soc. Am. B*, 1997, **14**, 1079–1087; (*d*) J. B. Ehrlich, X. L. Wu, I.-Y. S. Lee, Z.-Y. Hu, H. Rockel, S. R. Marder and J. W. Perry, *Opt. Lett.*, 1997, **22**, 1843–1845; (*e*) C. W. Spangler, *J. Mater. Chem.*, 1999, **9**, 2013–2020.

8 (*a*) D. A. Parthenopoulos and P. M. Rentzepis, *J. Appl. Phys.*, 1990, **68**, 5814–5818; (*b*) J. H. Strickler and W. W. Webb, *Opt. Lett.*, 1991, **16**, 1780–1782; (*c*) H. E. Pudavar, M. P. Joshi, P. N. Prasad and B. A. Reinhardt, *Appl. Phys. Lett.*, 1999, **74**, 1338–1340.

9 (*a*) J. D. Bhawalkar, J. Swiatkiewicz, S. J. Pan, J. K. Samarabandu, W. S. Liou, G. S. He, R. Berezney, P. C. Cheng and P. N. Prasad, *Scanning*, 1996, **18**, 562–566; (*b*) J. D. Bhawalkar, A. Shih, S. J. Pan, W. S. Liou, J. Swiatkiewicz, B. A. Reinhardt, P. N. Prasad and P. C. Cheng, *Bioimaging*, 1996, **4**, 168–178; (*c*) T. Gura, *Science*, 1997, **276**, 1988–1990; (*d*) X. Wang, L. J. Krebs, M. Al-Nuri, H. E. Pudavar, S. Ghosal, C. Liebow, A. A. Nagy, A. V. Schally and P. N. Prasad, *Proc. Natl. Acad. Sci. USA*, 1999, **96**, 11081.

10 J. D. Bhawalkar, N. D. Kumar, C. F. Zhao and P. N. Prasad, *J. Clinical Laser Medicine & Surgery*, 1997, **15**, 201–204.

11 (*a*) R. A. Negres, E. W. V. Stryland, D. J. Hagan, K. D. Belfield, K. J. Schafer, O. V. Przhonska and B. A. Reinhardt, *Proc. SPIE-Int. Soc. Opt. Eng.*, 1999, **3796**, 88; (*b*) R. A. Negres, J. M. Hales, A. Kobyakov, D. J. Hagan and E. W. V. Stryland, *Opt. Lett.*, 2002, **27**, 270.

12 D. A. Oulianov, I. V. Tomov, A. S. Dvornikov and P. M. Rentzepis, *Opt. Commun.*, 2001, **191**, 235–243.

13 (*a*) G. S. He, T.-C. Lin, P. N. Prasad, R. Kannan, R. A. Vaia and L.-S. Tan, *Opt. Express*, 2002, **10**, 566–574; (*b*) G. S. He, T.-C. Lin, P. N. Prasad, R. Kannan, R. A. Vaia and L.-S. Tan, *J. Phys. Chem. B*, 2002, **106**, 11081–11084.

14 (*a*) S. Bradamente and G. Pagani, *J. Chem. Soc., Perkin Trans. 2*, 1986, 1035–1046; (*b*) S. Bradamente and G. Pagani, *Pure Appl. Chem.*, 1989, **61**, 709–716; (*c*) A. Abbotto, S. Bradamente and G. Pagani, *J. Org. Chem.*, 1996, **61**, 1761–1769 (in the benzyl carbanions $PhCH^{-}X$ system, π-charge demand (c_x or q_x) is defined as the amount of π-charge that is transferred from the carbanionic carbon to the substituent group X. The reported data of charge demand for nitro, benzothiazole and alkylsulfonyl groups from these papers are $c_{nitro} = 0.567$, $c_{benzothiazole} = 0.316$ and $c_{alkylsulfonyl} = 0.269$, respectively. From ref. 14(*c*), by following the calculation process, the charge demand for oxazole can be obtained as $c_{oxazole} = 0.278$, which we assume should be reasonably close to the charge demand of oxadiazole.

15 (*a*) E. Lippert, *Z. Naturforsch., Teil A*, 1955, **10**, 541; (*b*) N. Mataga, Y. Kaifu and M. Koizuni, *Bull. Chem. Soc. Jpn.*, 1956, **29**, 465–470; (*c*) L. Onsaer, *J. Am. Chem. Soc.*, 1936, **58**, 1486–1493.

16 P. Fromherz, *J. Phys.Chem.*, 1995, **99**, 7188–7192.

17 J. W. Baur, M. D. Alexander J., M. Banach, L. R. Denny, B. A. Reinhardt and R. A. Vaia, *Chem. Mater.*, 1999, **11**, 2899–2906.

18 *CRC Handbook of Chemistry and Physics*; 71 edn., ed. D. R Lide, CRC press, Boca Raton, 1990.

19 M. Ravi, T. Soujanya, A. Samanta and T. P. Radhakrishnan, *J. Chem. Soc., Faraday Trans.*, 1995, **91**, 2739–2742.